# *Supporting Information*

# Non-mutagenic Ru(II)-phosphine-based Complexes Induce Mitochondria-mediated Apoptosis in Breast Cancer Cells: From 2D to 3D Investigations

*Marcos V. Palmeira-Mello,*[1] Tamara Teixeira,[1] Analu R. Costa,[1,2] Aline Maria Machado,[3] Rone A. De Grandis,[4] Leticia P. de Oliveira,[1] Carlos A. F. Moraes,[1] João H. de Araujo-Neto,[5] Victor M. Deflon,[6] Adriano D. Andricopulo,[2] Javier Ellena,[7] Heloisa S. Selistre-de-Araújo,[3] Fillipe V. Rocha,[1] and Alzir A. Batista*[1]*

[1] *Departament of Chemistry, Universidade Federal de São Carlos (UFSCar), São Carlos, 13565-905, SP, Brazil*

[2] *Laboratory of Medicinal and Computational Chemistry (LQMC), Institute of Physics, Universidade de São Paulo (USP), São Carlos, 13563-120, SP, Brazil.*

[3] *Department of Physiological Sciences, Universidade Federal de São Carlos (UFSCar), São Carlos, 13565-905, SP, Brazil*

[4] *School of Pharmaceutical Sciences of São Paulo State University (UNESP), Araraquara, 14800-903, SP, Brazil.*

[5] *Department of Fundamental Chemistry, Institute of Chemistry, University of São Paulo. 05508-000 São Paulo, SP, Brazil.*

[6] *São Carlos Institute of Chemistry, Universidade de São Paulo (USP), São Carlos, 13566-590, SP, Brazil.*

[7] *São Carlos Institute of Physics, Universidade de São Paulo (USP), São Carlos, 13566-590, SP, Brazil.*

*Corresponding authors: Marcos Palmeira-Mello (marcos.palmeira@ufscar.br, ORCID 0000-0003-2550-5315), and Alzir Batista (daab@ufscar.br, ORCID 0000-0002-4671-2754).

# Table of Content

## Part I – IR spectra

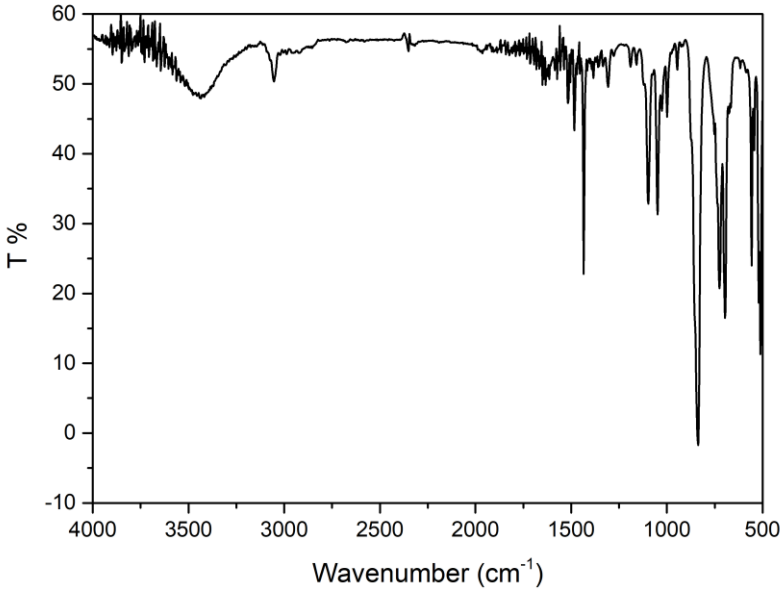


**Fig. S1** IR spectrum of complex $[Ru(mtz)(dppm)_2]PF_6$ (**Ru1**) in KBr.

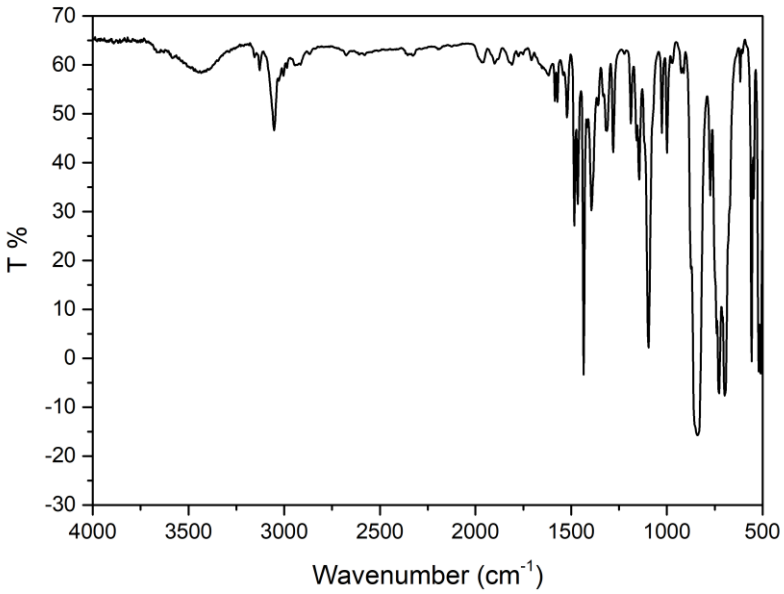


**Fig. S2** IR spectrum of complex $[Ru(mmi)(dppm)_2]PF_6$ (**Ru2**) in KBr.

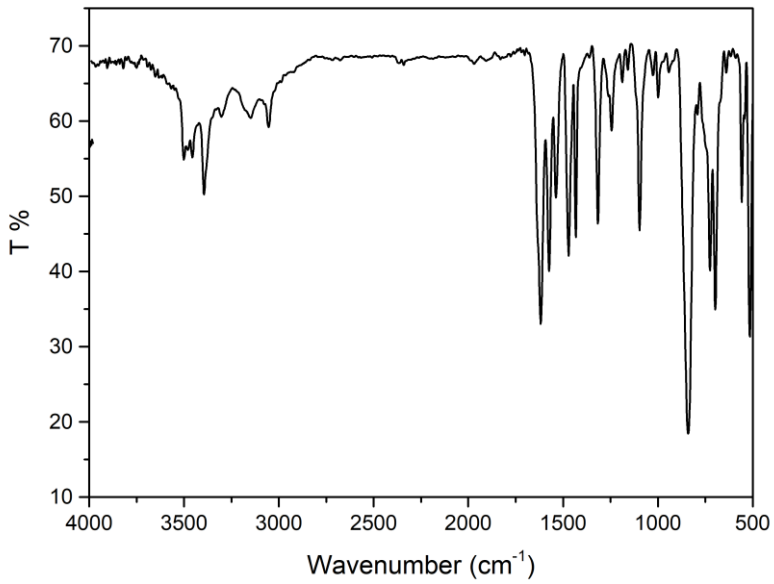


**Fig. S3** IR spectrum of complex $[Ru(dmp)(dppm)_2]PF_6$ (**Ru3**) in KBr.

## Part II – NMR spectra and 2D correlation maps

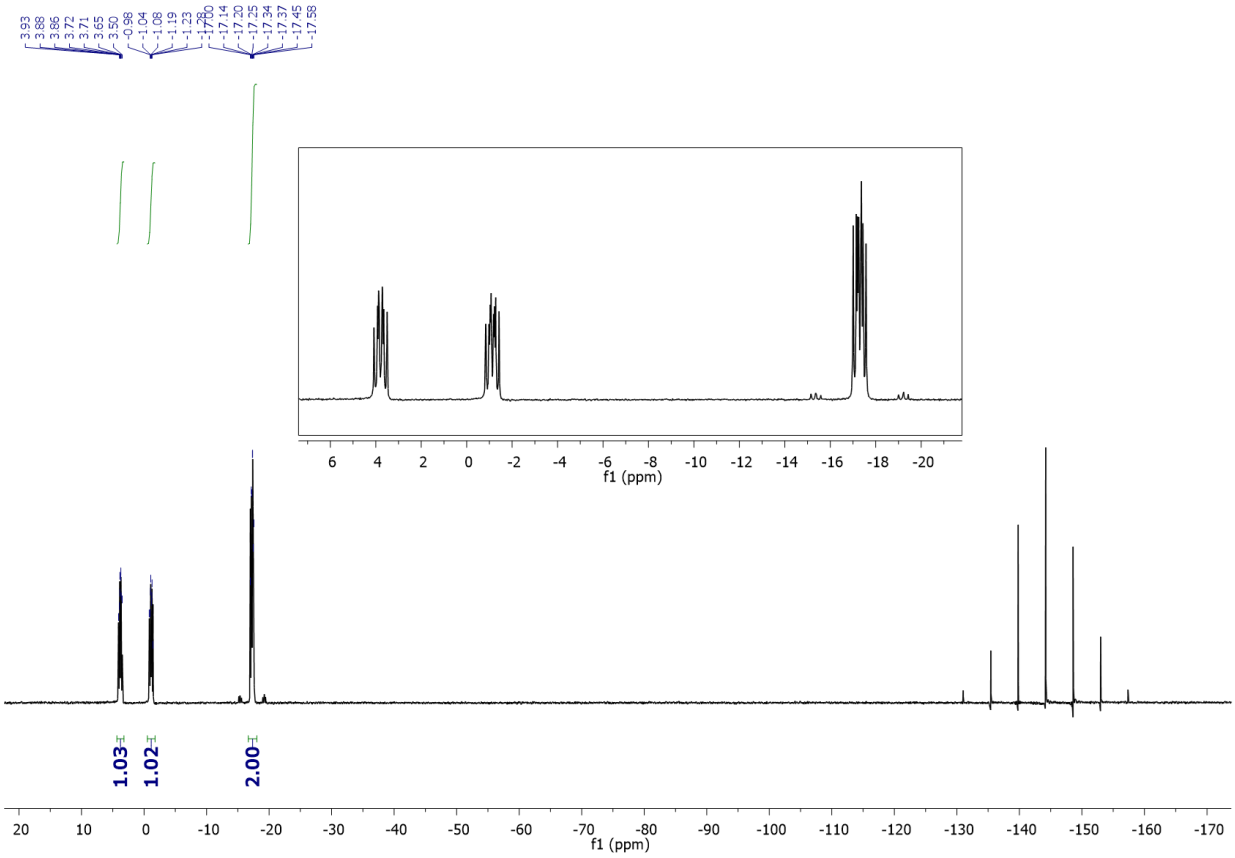


**Fig. S4** $^{31}P\ \{^{1}H\}$ NMR spectrum of complex $[Ru(mtz)(dppm)_2]PF_6$ (**Ru1**) in $CH_2Cl_2/D_2O$ at 298 K.

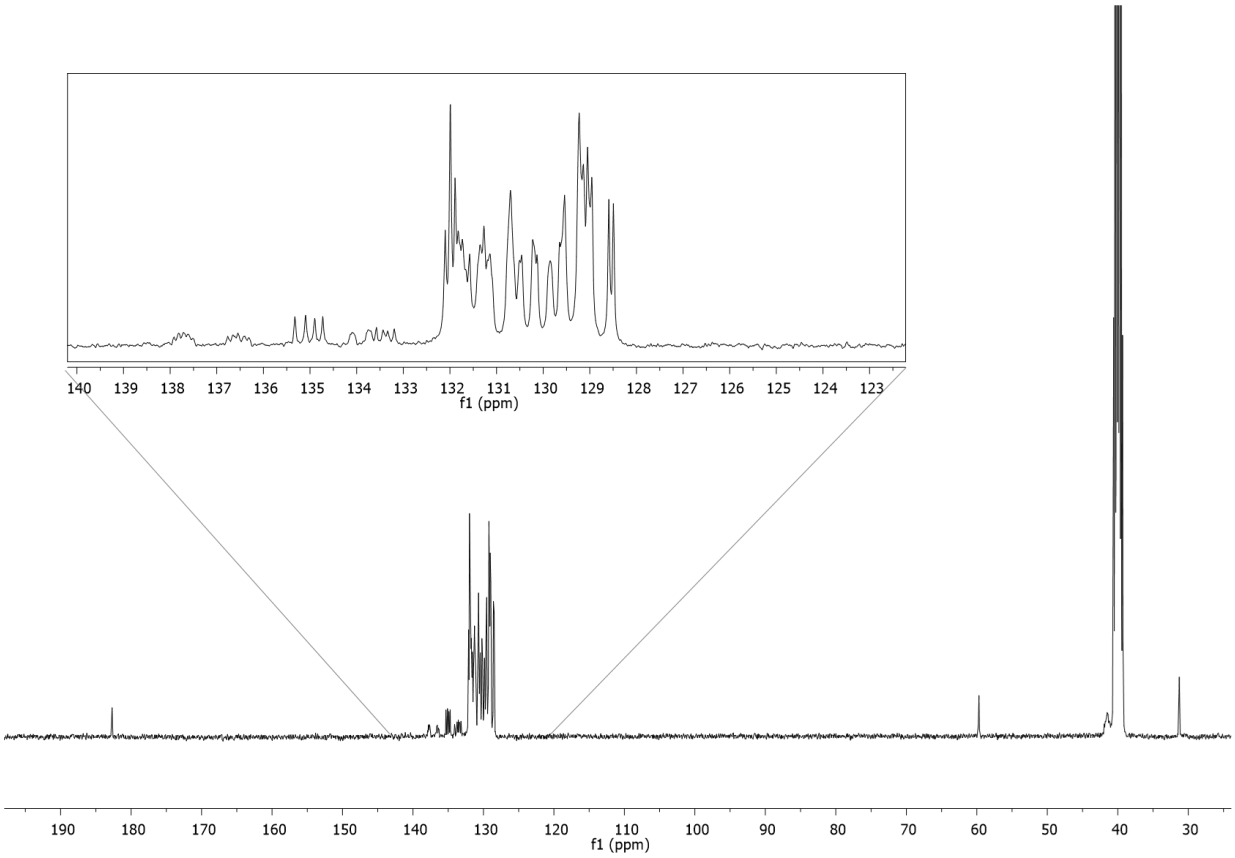


**Fig. S5** $^{13}C\ \{^{1}H\}$ NMR spectrum of $[Ru(mtz)(dppm)_2]PF_6$ (**Ru1**) in DMSO-$d_6$ at 298K.

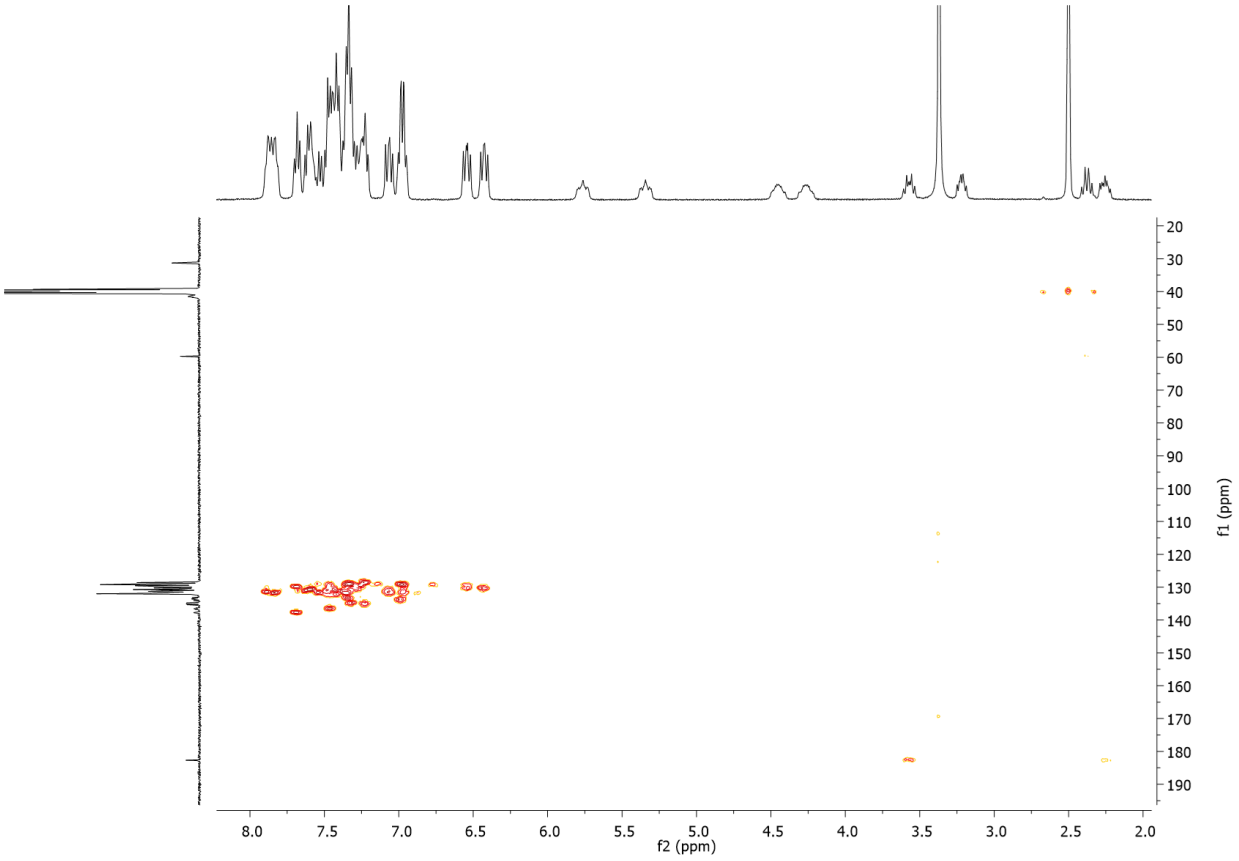


**Fig. S6** $^{1}H$-$^{13}C$ HMBC NMR correlation map of $[Ru(mtz)(dppm)_2]PF_6$ (**Ru1**) in DMSO-$d_6$ at 298K.

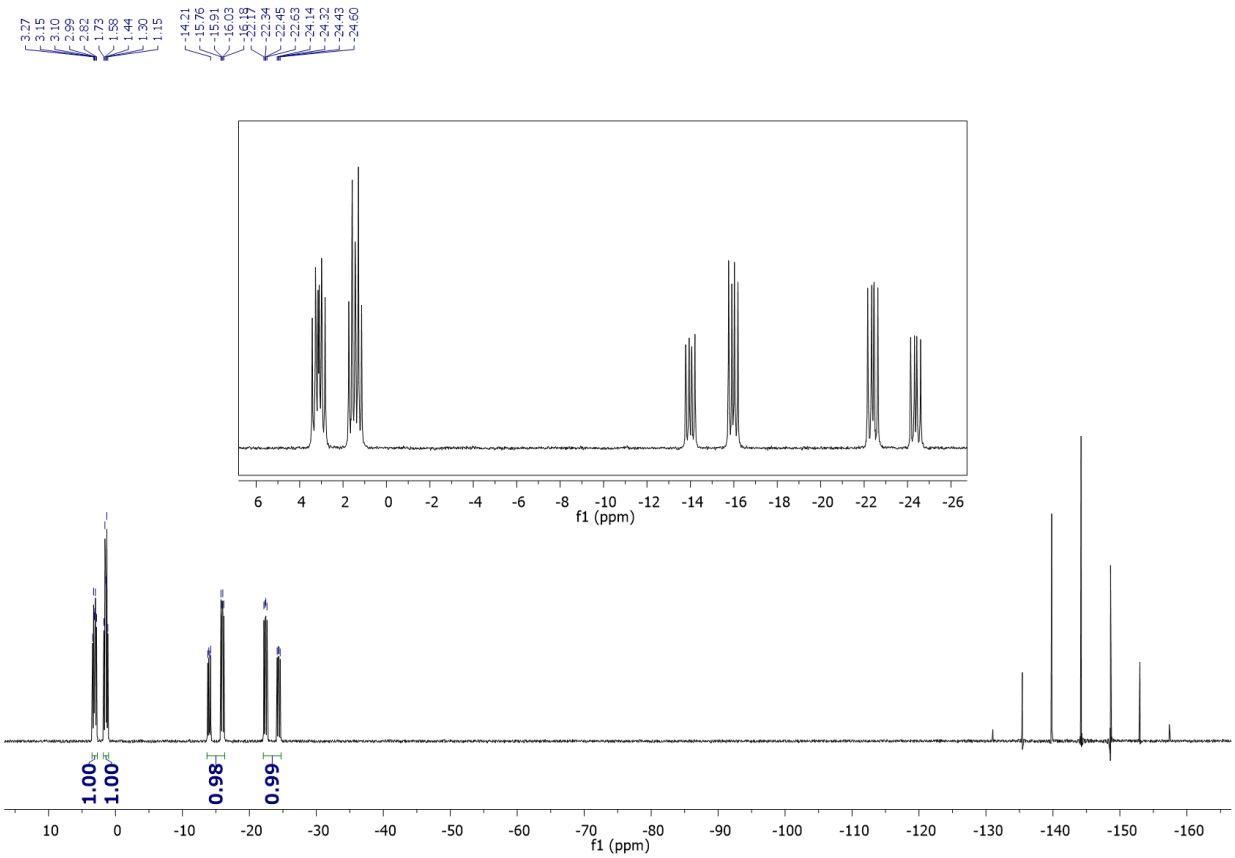


**Fig. S7** $^{31}P\ \{^{1}H\}$ NMR spectrum of complex $[Ru(mmi)(dppm)_2]PF_6$ (**Ru2**) in $CH_2Cl_2/D_2O$ at 298 K.

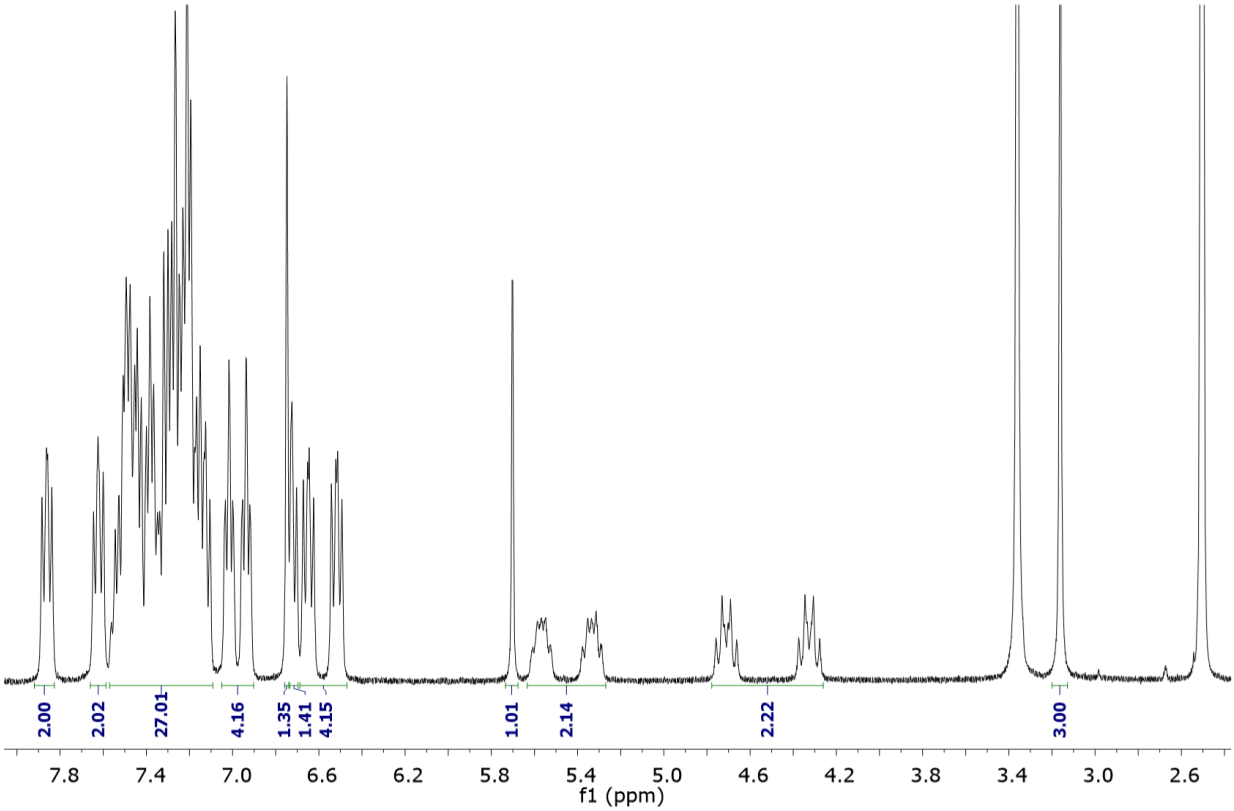


**Fig. S8** $^{1}$H NMR spectrum of complex $[Ru(mmi)(dppm)_2]PF_6$ (**Ru2**) in DMSO-$d_6$ at 298 K.

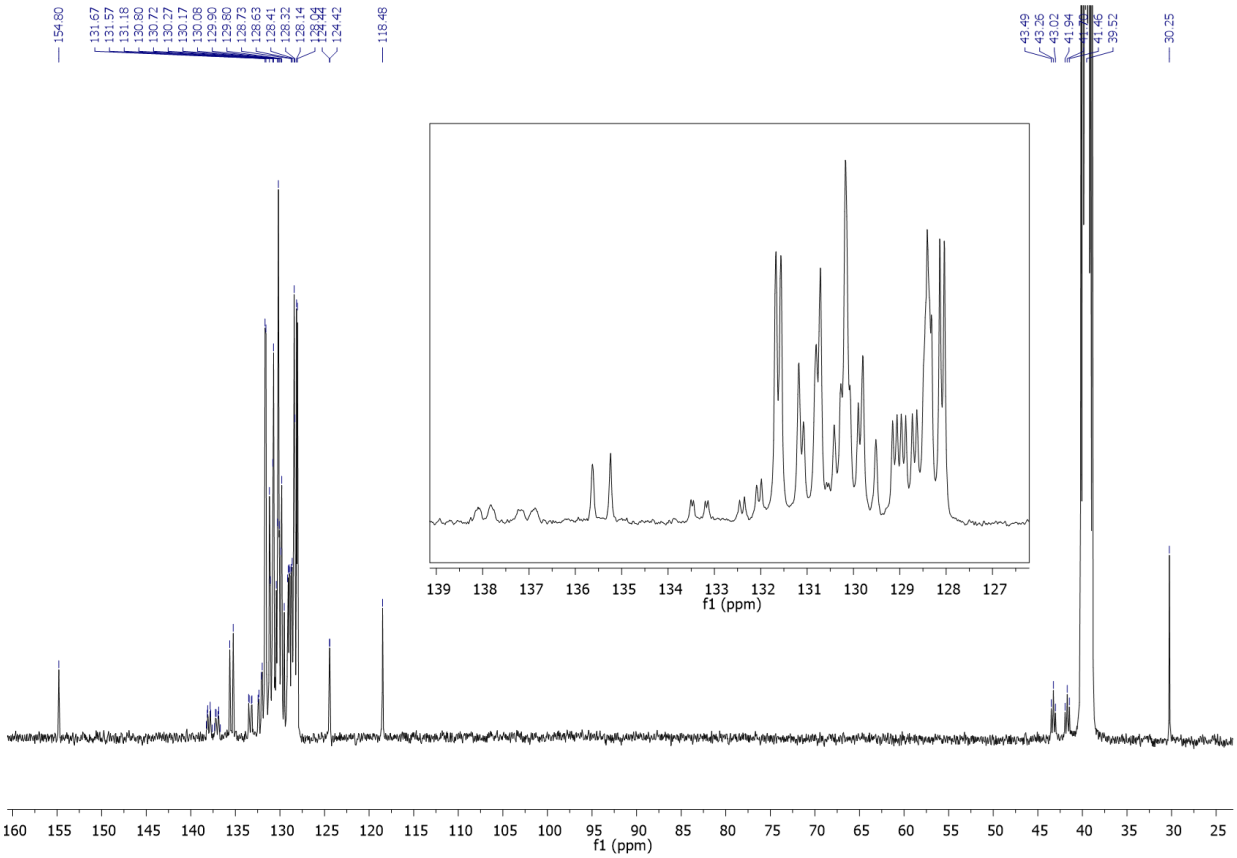


**Fig. S9** $^{13}C\ \{^{1}H\}$ NMR spectrum of $[Ru(mmi)(dppm)_2]PF_6$ (**Ru2**) in DMSO-$d_6$ at 298K.

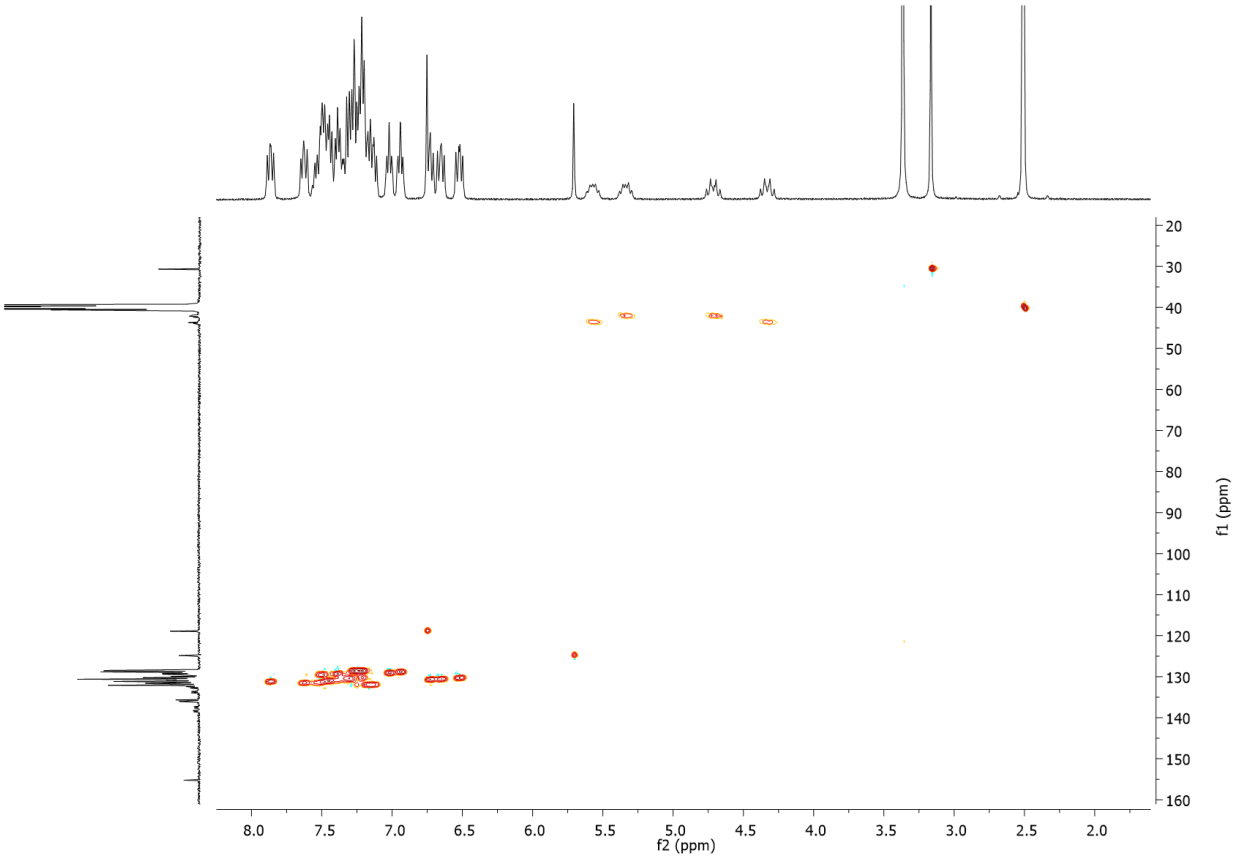


**Fig. S10** $^{1}H$-$^{13}C$ HSQC NMR correlation map of $[Ru(mmi)(dppm)_2]PF_6$ (**Ru2**) in DMSO-$d_6$ at 298K.

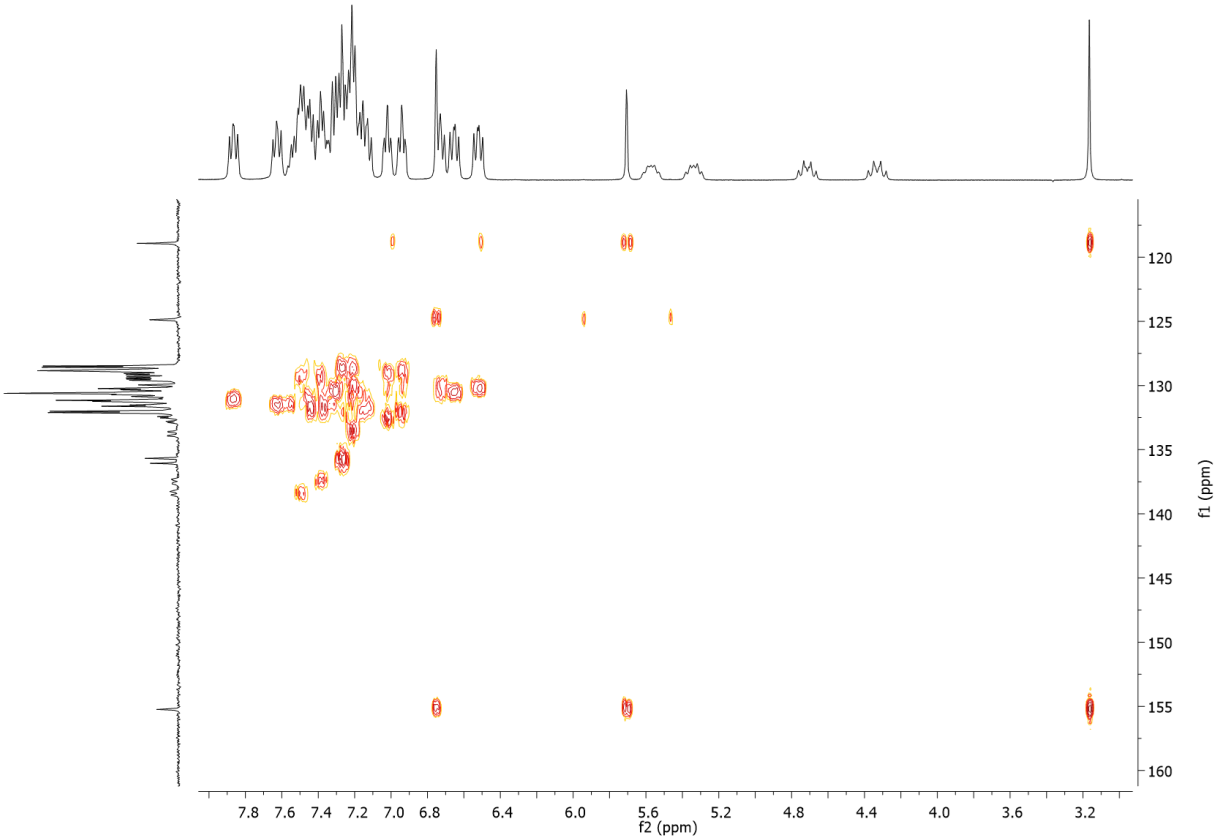


**Fig. S11** $^{1}H$-$^{13}C$ HMBC NMR correlation map of $[Ru(mmi)(dppm)_2]PF_6$ (**Ru2**) in DMSO-$d_6$ at 298K.

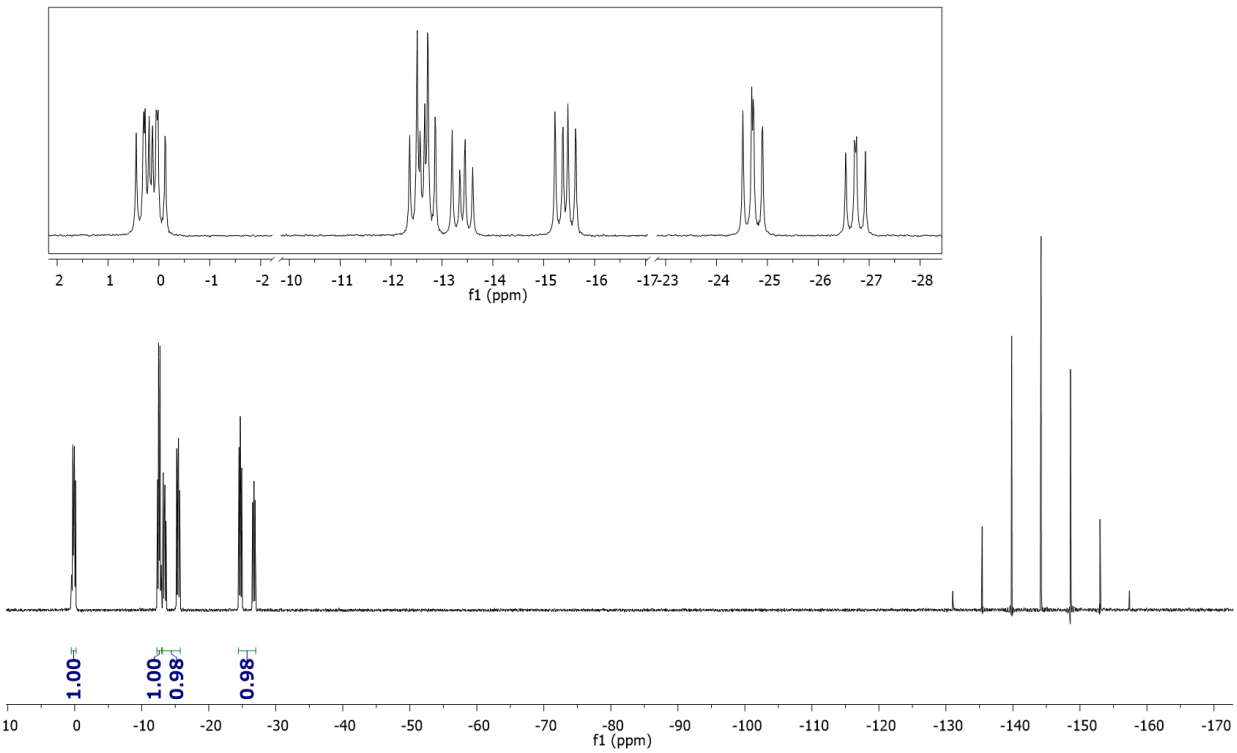


**Fig. S12** $^{31}P\ \{^{1}H\}$ NMR spectrum of complex $[Ru(dmp)(dppm)_2]PF_6$ (**Ru3**) in $CH_2Cl_2/D_2O$ at 298 K.

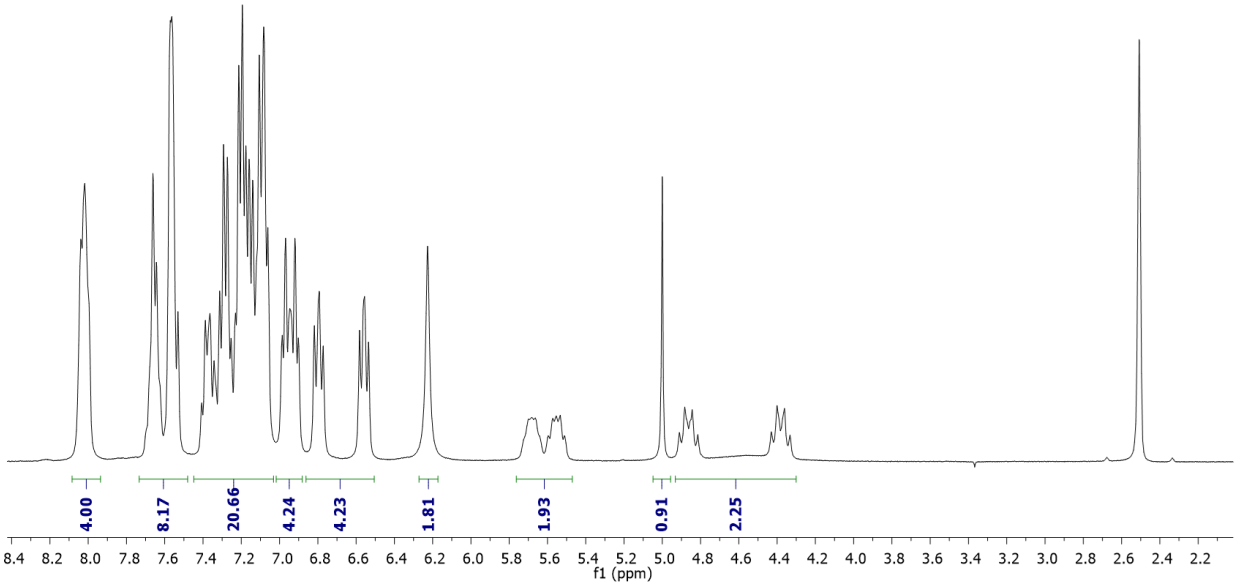


**Fig. S13** $^{1}$H NMR spectrum of complex [Ru(dmp)(dppm)$_2$]PF$_6$ (**Ru3**) in DMSO-d$_6$ at 298 K.

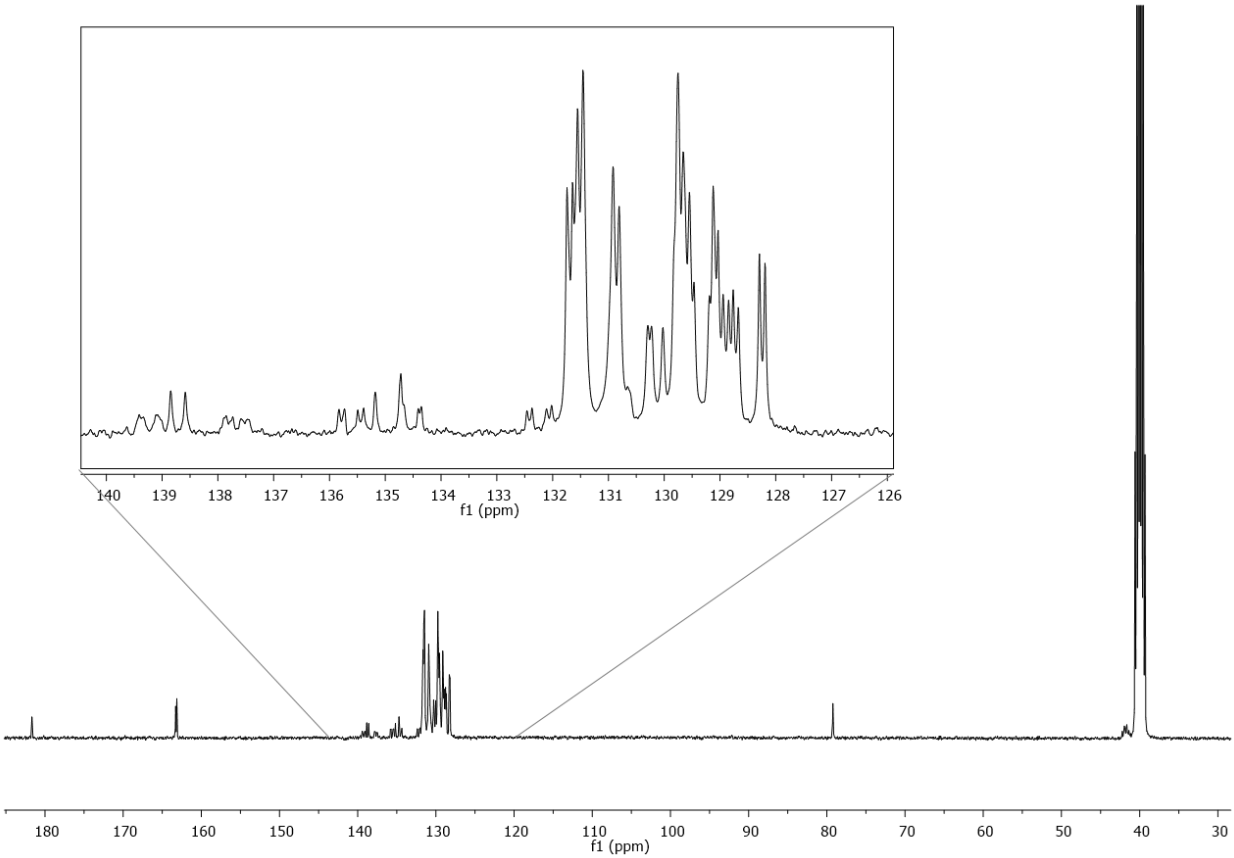


**Fig. S14** $^{13}C\ \{^{1}H\}$ NMR spectrum of $[Ru(dmp)(dppm)_2]PF_6$ (**Ru3**) in DMSO-$d_6$ at 298K.

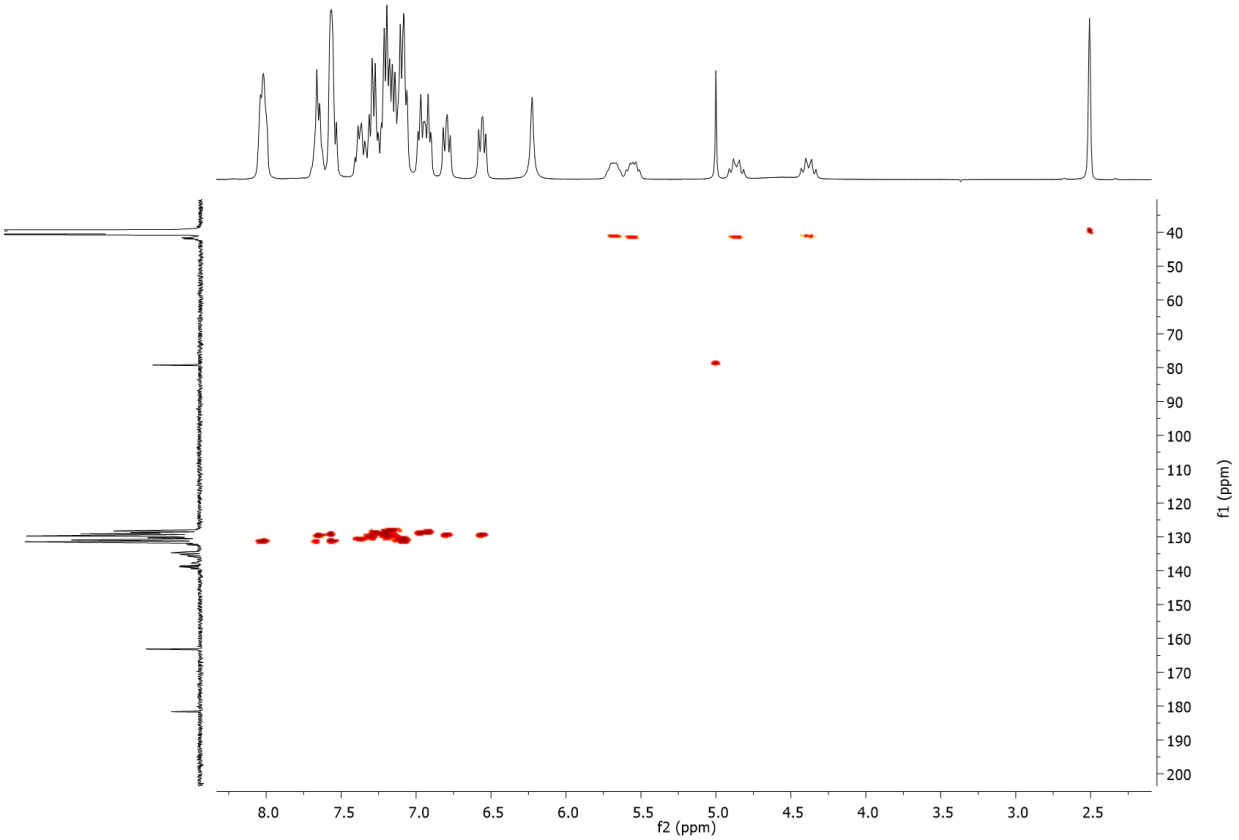


**Fig. S15** $^{1}H$-$^{13}C$ HSQC NMR correlation map of $[Ru(dmp)(dppm)_2]PF_6$ (**Ru3**) in DMSO-$d_6$ at 298K.

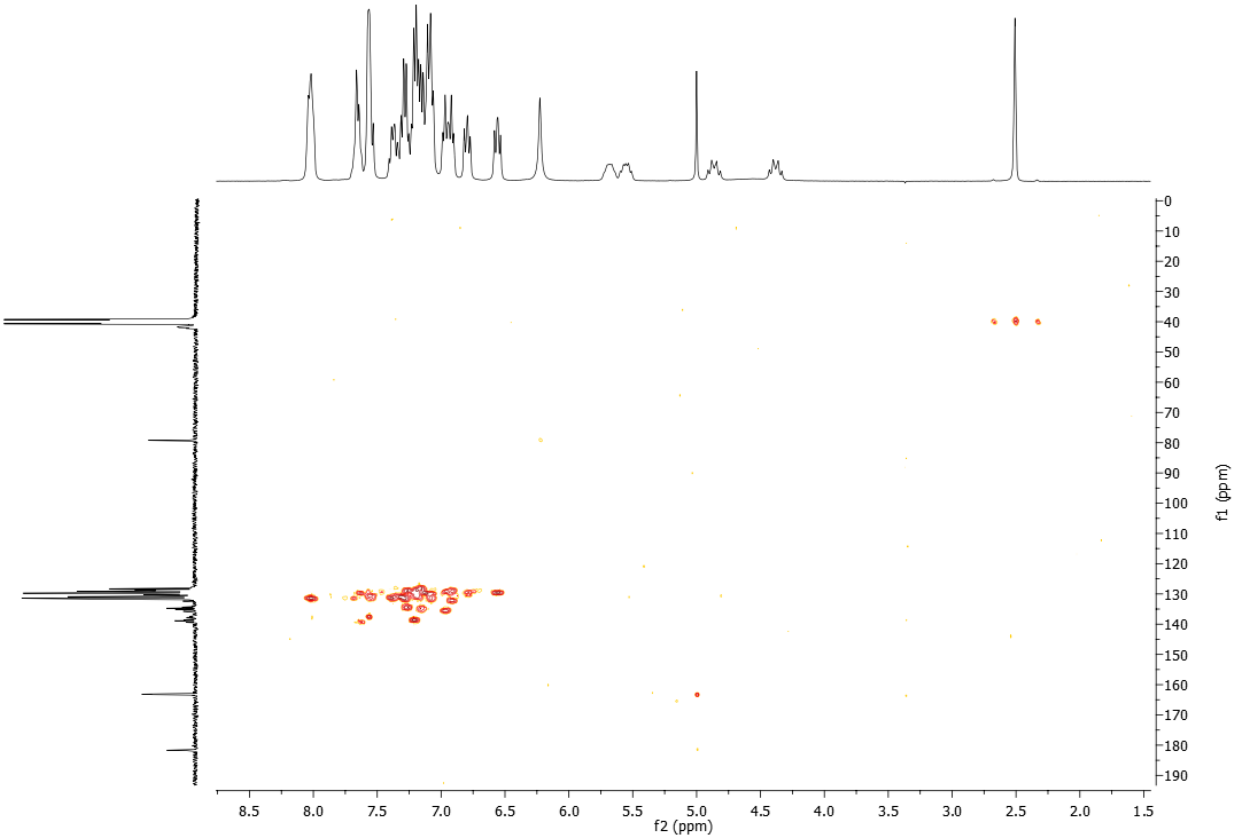


**Fig. S16** $^{1}H$-$^{13}C$ HMBC NMR correlation map of $[Ru(dmp)(dppm)_2]PF_6$ (**Ru3**) in DMSO-$d_6$ at 298K.

## Part III – UV-Vis spectra

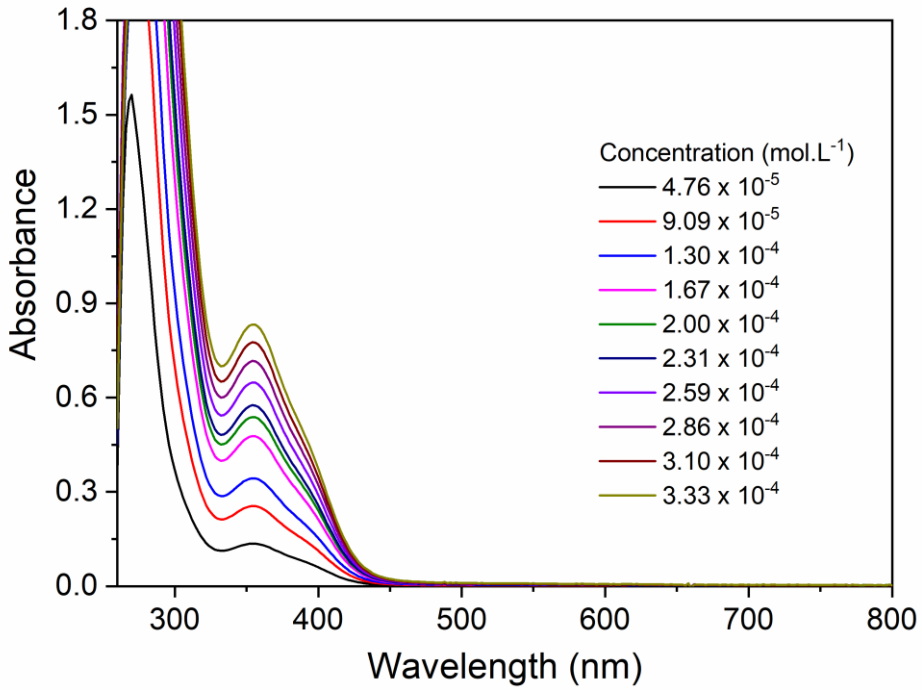


**Fig. S17** UV-Vis spectrum of $[Ru(mtz)(dppm)_2]PF_6$ (**Ru1**) in DMSO-$d_6$.

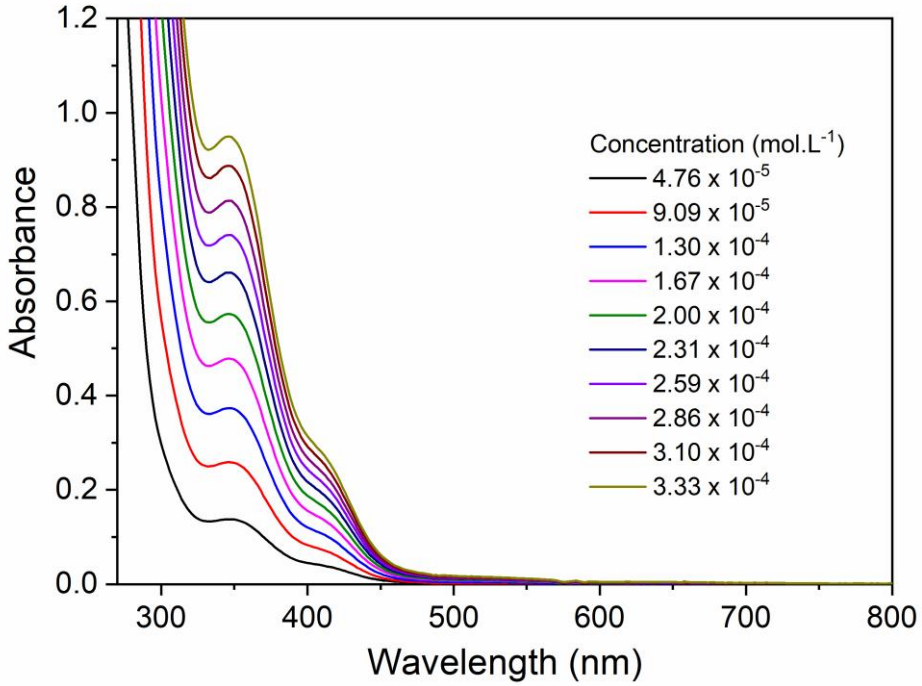


**Fig. S18** UV-Vis spectrum of $[Ru(mmi)(dppm)_2]PF_6$ (**Ru2**) in DMSO-$d_6$.

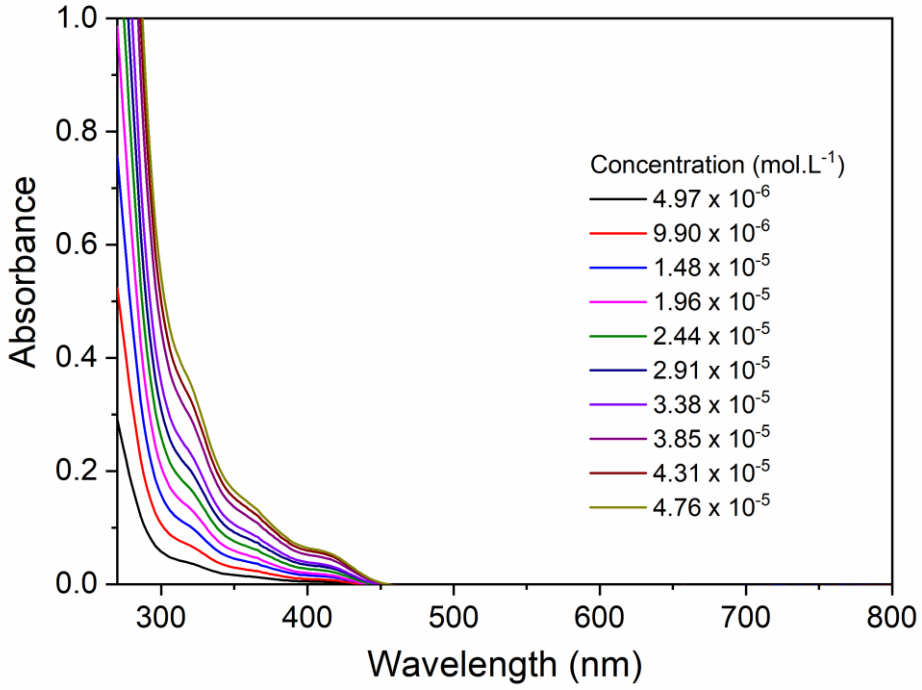


**Fig. S19** UV-Vis spectrum of $[Ru(dmp)(dppm)_2]PF_6$ (**Ru3**) in DMSO-$d_6$.

## Part IV – Mass Spectrometry

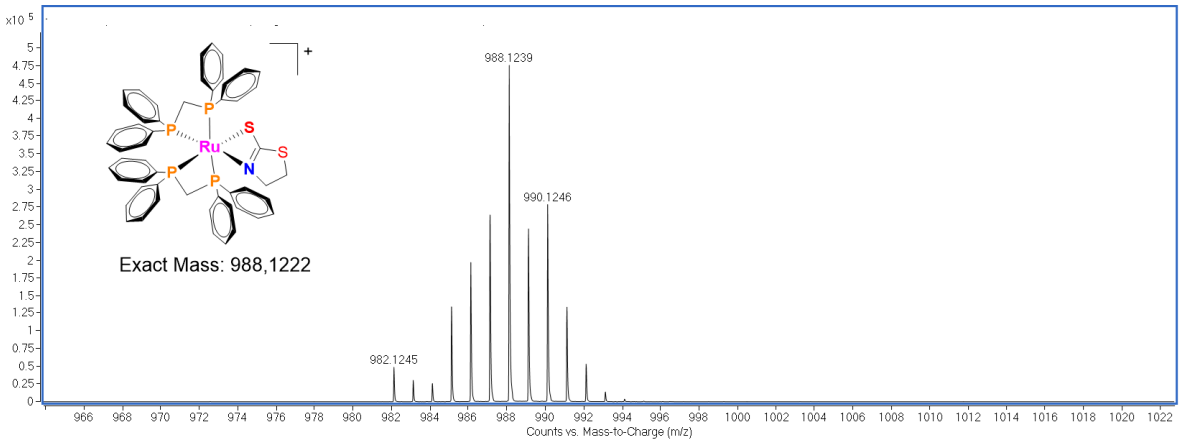


**Fig. S20** MS spectrum of $[Ru(mtz)(dppm)_2]PF_6$ (**Ru1**).

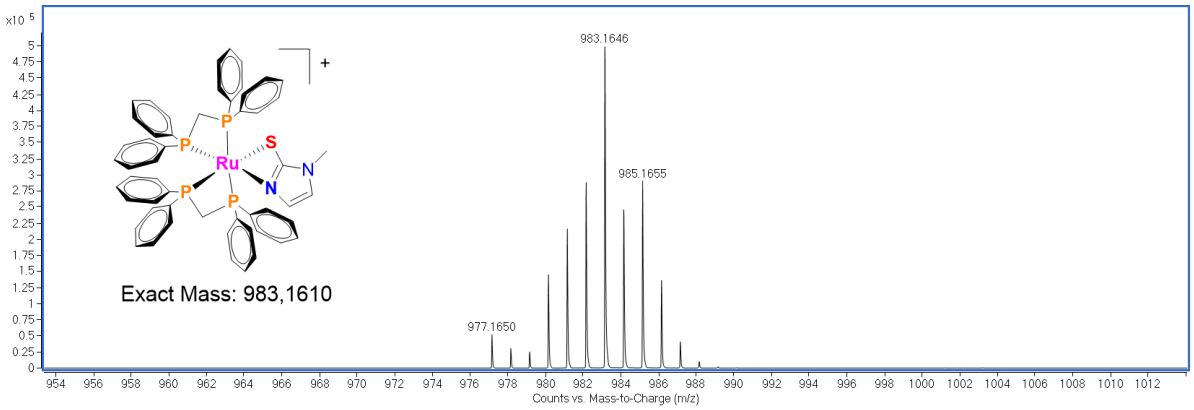


**Fig. S21** MS spectrum of $[Ru(mmi)(dppm)_2]PF_6$ (**Ru2**).

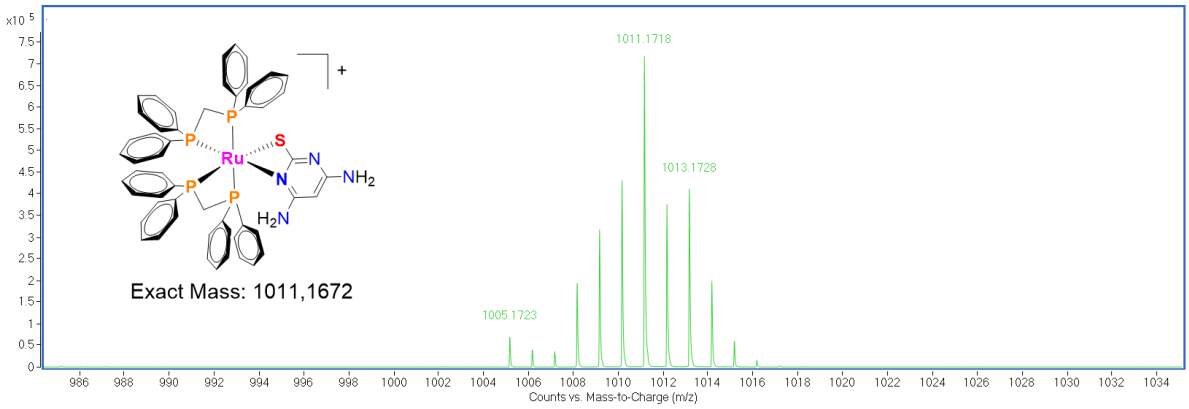


**Fig. 22** MS spectrum of $[Ru(dmp)(dppm)_2]PF_6$ (**Ru3**).

## Part V – Electrochemical data

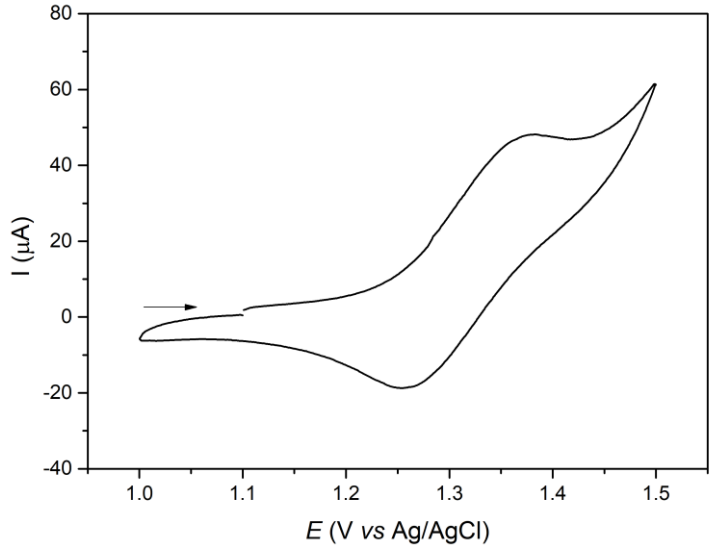


**Fig. S23** Cyclic voltammogram of $[Ru(mtz)(dppm)_2]PF_6$ (**Ru1**) in $CH_2Cl_2$ (0.1 mol $L^{-1}$ TBAP). Scan rate 50 mV $s^{-1}$.

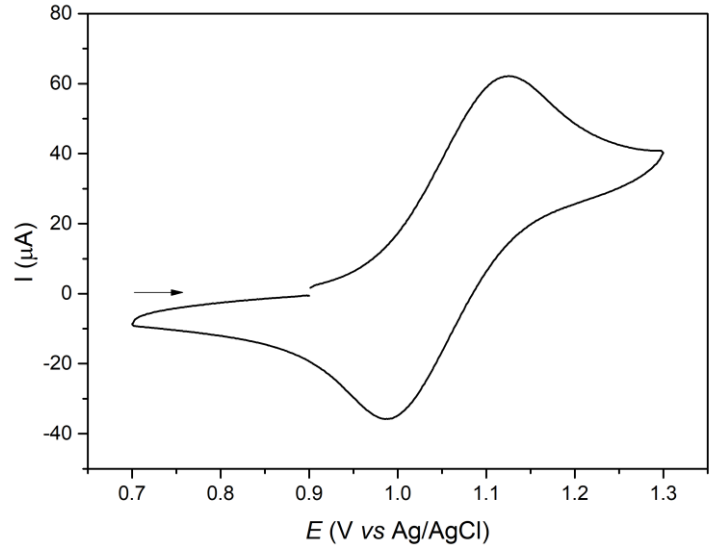


**Fig. S24** Cyclic voltammogram of $[Ru(mmi)(dppm)_2]PF_6$ (**Ru2**) in $CH_2Cl_2$ (0.1 mol $L^{-1}$ TBAP). Scan rate 50 mV $s^{-1}$.

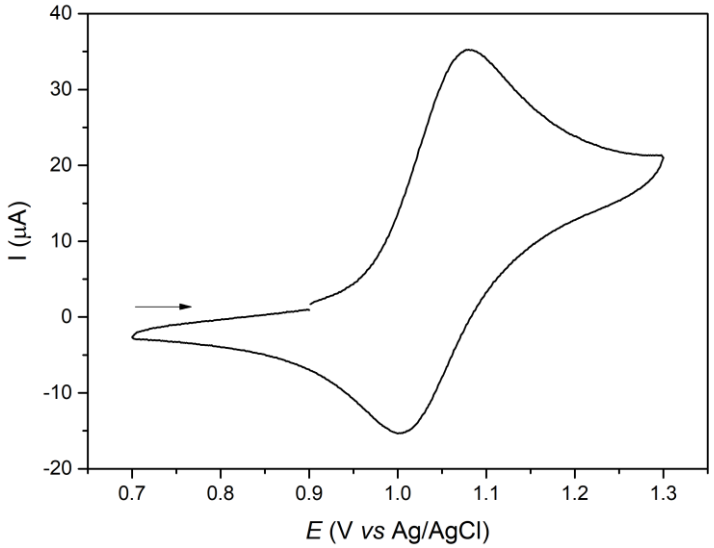


**Fig. S25** Cyclic voltammogram of $[Ru(dmp)(dppm)_2]PF_6$ (**Ru3**) in $CH_2Cl_2$ (0.1 mol $L^{-1}$ TBAP). Scan rate 50 mV $s^{-1}$.

**Table S1** Electrochemical data of the complexes (**Ru1**–**Ru3**) in DCM/$TBAClO_4$ 0.1 M solutions, using a three-electrode setup (working: carbon; ref.: Ag/AgCl; aux.: Pt wire). Scan rate: 50 mV $s^{-1}$.

| Complex | $E_{pa}$ (V) | $E_{pc}$ (V) | $\Delta E$ (V) | $E_{1/2}$ (V) |
|---|---|---|---|---|
| **Ru1** | 1.38 | 1.25 | 0.13 | 1.32 |
| **Ru2** | 1.12 | 0.98 | 0.14 | 1.05 |
| **Ru3** | 1.08 | 1.00 | 0.08 | 1.04 |

## Part VI – X-Ray Diffraction

**Table S2** C The bond distance and angles of **Ru1–Ru3**

| | Ru1 | Ru2* | Ru3 |
|---|---|---|---|
| | | Bond Distance (Å) | |
| Ru-S1 | 2.485(1) | 2.54(2) / 2.58(2) | 2.432(1) |
| Ru-N1 | 2.147(2) | 2.11(2) / 2.08(2) | 2.191(1) |
| Ru-P1 | 2.395(1) | 2.310(1) | 2.373(1) |
| Ru-P2 | 2.313(1) | 2.372(1) | 2.305(1) |
| Ru-P3 | 2.319(1) | 2.299(1) | 2.340(1) |
| Ru-P4 | 2.316(1) | 2.341(1) | 2.353(1) |
| C1-S1 | 1.712(3) | 1.76(2) / 1.80(2) | 1.732(2) |
| | | Bond Angle (°) | |
| S1-Ru-N1 | 66.28(7) | 66.3(3) / 66.7(4) | 66.42(5) |
| P1-Ru-P2 | 71.70(3) | 71.33(4) | 72.12(2) |
| P3-Ru-P4 | 72.32(3) | 71.88(4) | 71.19(2) |

* This complex exhibit disorder in the coordination of the ligand, which was refined in two positions.

**Table S3** Crystallographic data of the complexes **Ru1–Ru3**

| | **Ru1** | **Ru2** | **Ru3** |
|---|---|---|---|
| CCDC code | 2235452 | 2235453 | 2235454 |
| Empirical formula | $C_{53}H_{48}F_6NP_5RuS_2$ | $C_{54}H_{49}F_6N_2P_5RuS$ | $C_{54}H_{49}F_6N_4P_5RuS$ |
| Formula weight | 1132.96 | 1127.93 | 1155.95 |
| Temperature/K | 296(2) | 100(2) | 296.15 |
| Crystal system | monoclinic | Monoclinic | Triclinic |
| Space group | P21/n | C2/c | P-1 |
| a/Å | 11.3460(4) | 34.440(3) | 11.4598(3) |
| b/Å | 21.2268(7) | 12.0353(11) | 11.8082(4) |
| c/Å | 22.2419(7) | 25.210(2) | 21.7901(7) |
| α/° | 90 | 90 | 103.4800(10) |
| β/° | 94.1000(10) | 92.977(9) | 93.5460(10) |
| γ/° | 90 | 90 | 111.4500(10) |
| Volume/Å$^3$ | 5343.0(3) | 10435.4(16) | 2633.31(14) |
| Z | 4 | 8 | 2 |
| $\rho_{calc}$g/cm$^3$ | 1.408 | 1.436 | 1.458 |
| μ/mm$^{-1}$ | 0.578 | 0.554 | 0.551 |
| F(000) | 2312 | 4608 | 1180 |
| Crystal size/mm$^3$ | 0.14 × 0.09 × 0.05 | 0.40 × 0.25 × 0.10 | 0.16 × 0.07 × 0.04 |
| Radiation | MoKα (λ = 0.71073) | Mo Kα (λ = 0.71073) | MoKα (λ = 0.71073) |
| 2Θ range for data collection/° | 2.656 to 52.784 | 5.108 to 51.362 | 3.81 to 52.942 |
| Index ranges | -13 ≤ h ≤ 14, -26 ≤ k ≤ 26, -27 ≤ l ≤ 27 | -40 ≤ h ≤ 41, -14 ≤ k ≤ 14, -30 ≤ l ≤ 30 | -14 ≤ h ≤ 14, -14 ≤ k ≤ 14, -27 ≤ l ≤ 27 |
| Reflections collected | 91596 | 33322 | 101959 |
| Independent reflections | 10952 [$R_{int}$ = 0.0403, $R_{sigma}$ = 0.0239] | 9908 [$R_{int}$ = 0.0766, $R_{sigma}$ = 0.0938] | 10841 [$R_{int}$ = 0.0394, $R_{sigma}$ = 0.0224] |
| Data/restraints/ parameters | 10952/0/607 | 9908/151/714 | 10841/0/563 |
| Goodness-of-fit on F$^2$ | 1.057 | 1.024 | 1.046 |
| Final R indexes [I>=2σ (I)] | R1 = 0.0409, wR2 = 0.0964 | $R_1$ = 0.0508, $wR_2$ = 0.0897 | $R_1$ = 0.0333, $wR_2$ = 0.0831 |
| R indexes [all data] | R1 = 0.0531, wR2 = 0.1049 | $R_1$ = 0.1031, $wR_2$ = 0.1141 | $R_1$ = 0.0409, $wR_2$ = 0.0889 |
| Largest diff. peak/hole / eÅ$^{-3}$ | 0.86/-0.50 | 0.57/-0.39 | 0.51/-0.36 |

## Part VII – Stability in solution

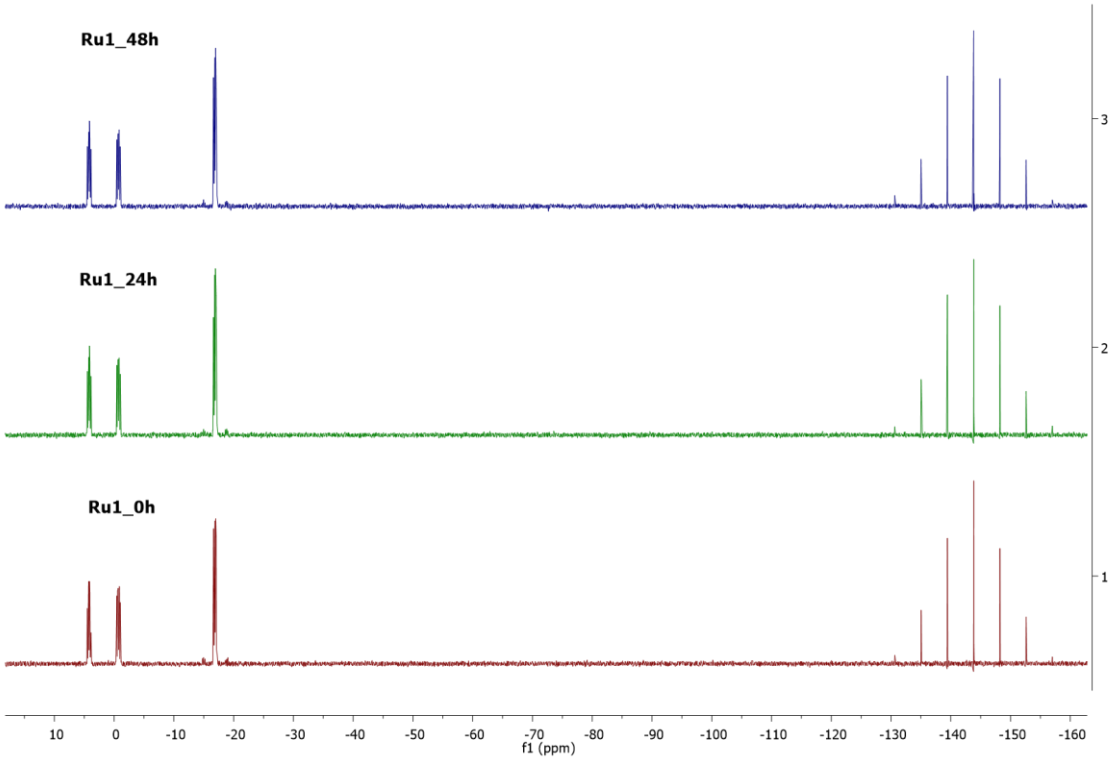


**Fig. S26** $^{31}P\ \{^{1}H\}$ NMR spectra of complex $[Ru(mtz)(dppm)_2]PF_6$ (**Ru1**) in DMSO at different times: 0 h, 24 h and 48 h.

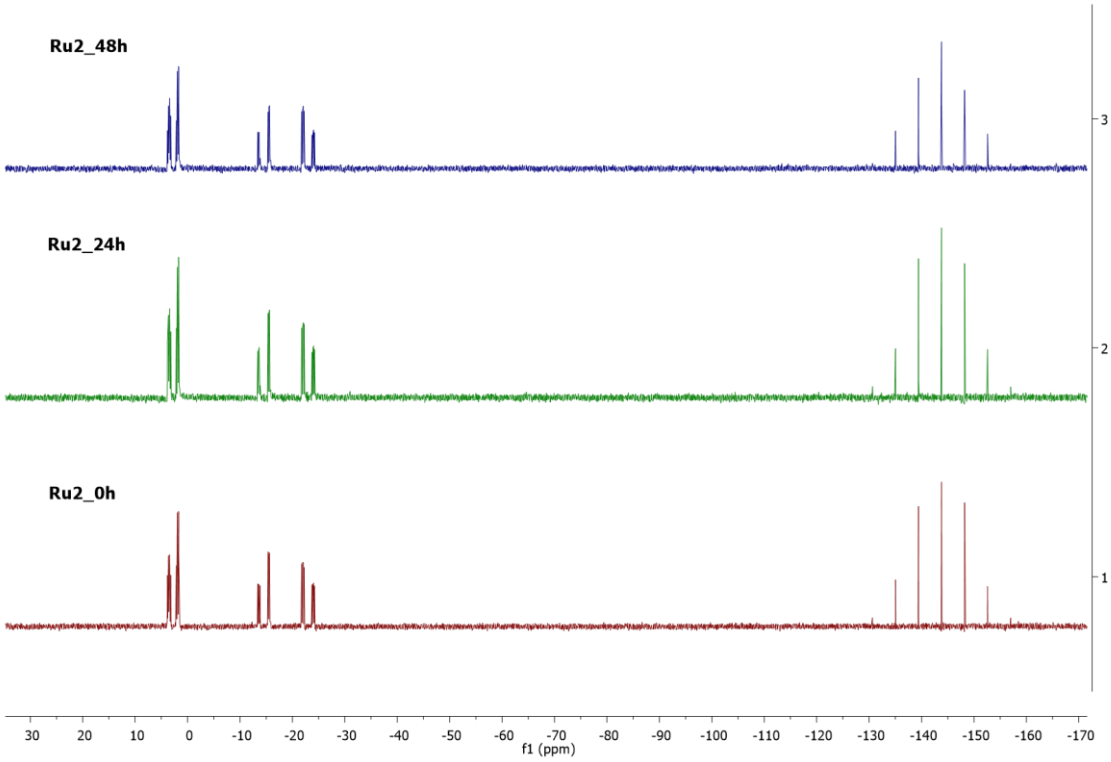


**Fig. S27** $^{31}P\ \{^{1}H\}$ NMR spectra of complex $[Ru(mmi)(dppm)_2]PF_6$ (**Ru2**) in DMSO at different times: 0 h, 24 h and 48 h.

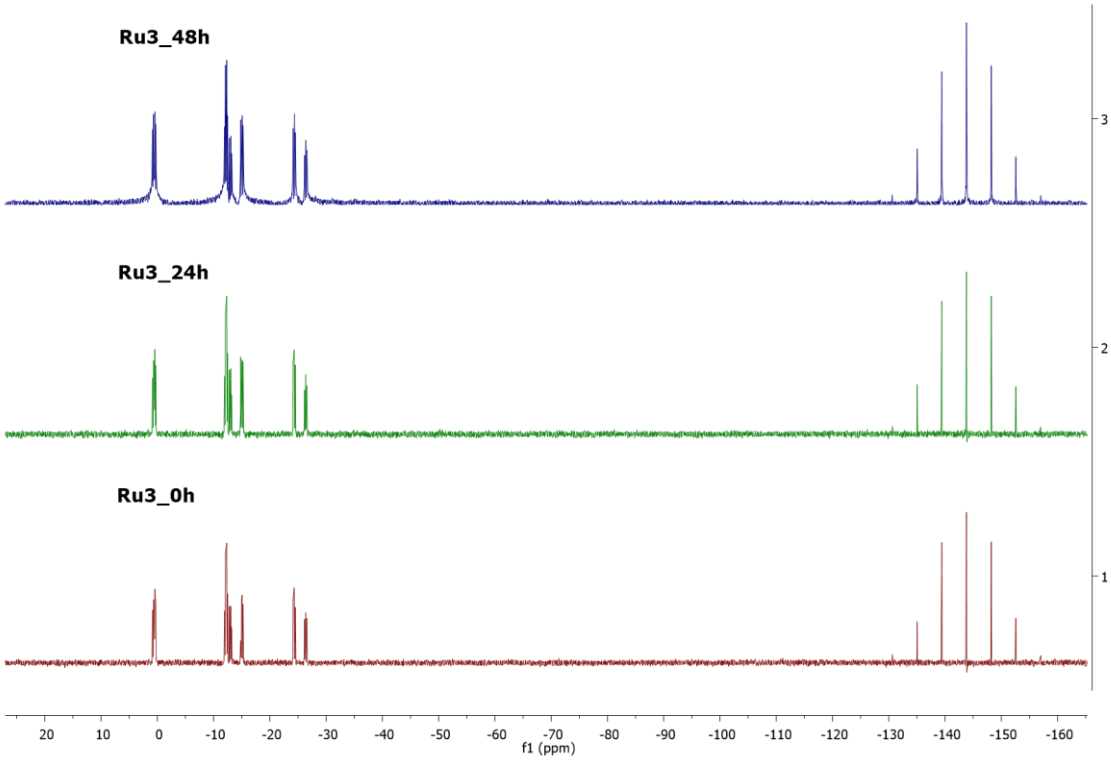


**Fig. S28** $^{31}P\ \{^{1}H\}$ NMR spectra of complex $[Ru(dmp)(dppm)_2]PF_6$ (**Ru3**) in DMSO at different times: 0 h, 24 h and 48 h.

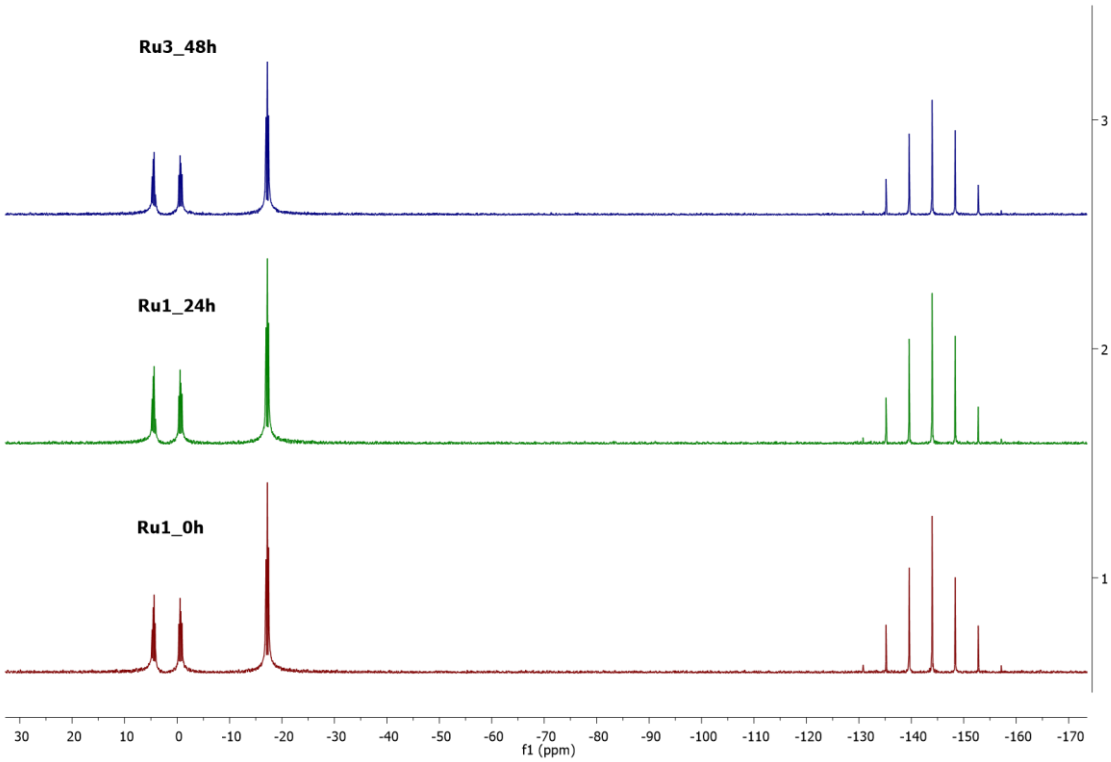


**Fig. S29** $^{31}P\ \{^{1}H\}$ NMR spectra of complex $[Ru(mtz)(dppm)_2]PF_6$ (**Ru1**) in DMSO/DMEM (90:10) at different times: 0 h, 24 h and 48 h.

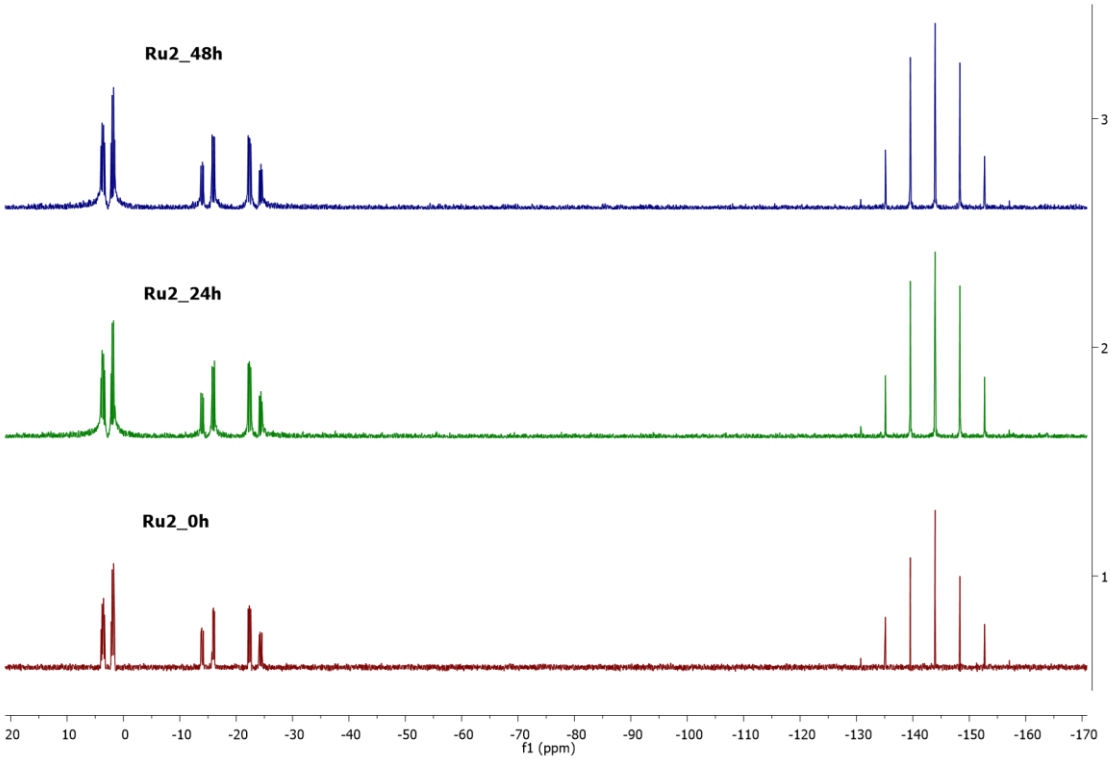


**Fig. S30** $^{31}P\ \{^{1}H\}$ NMR spectra of complex $[Ru(mmi)(dppm)_2]PF_6$ (**Ru2**) in DMSO/DMEM (90:10) at different times: 0 h, 24 h and 48 h.

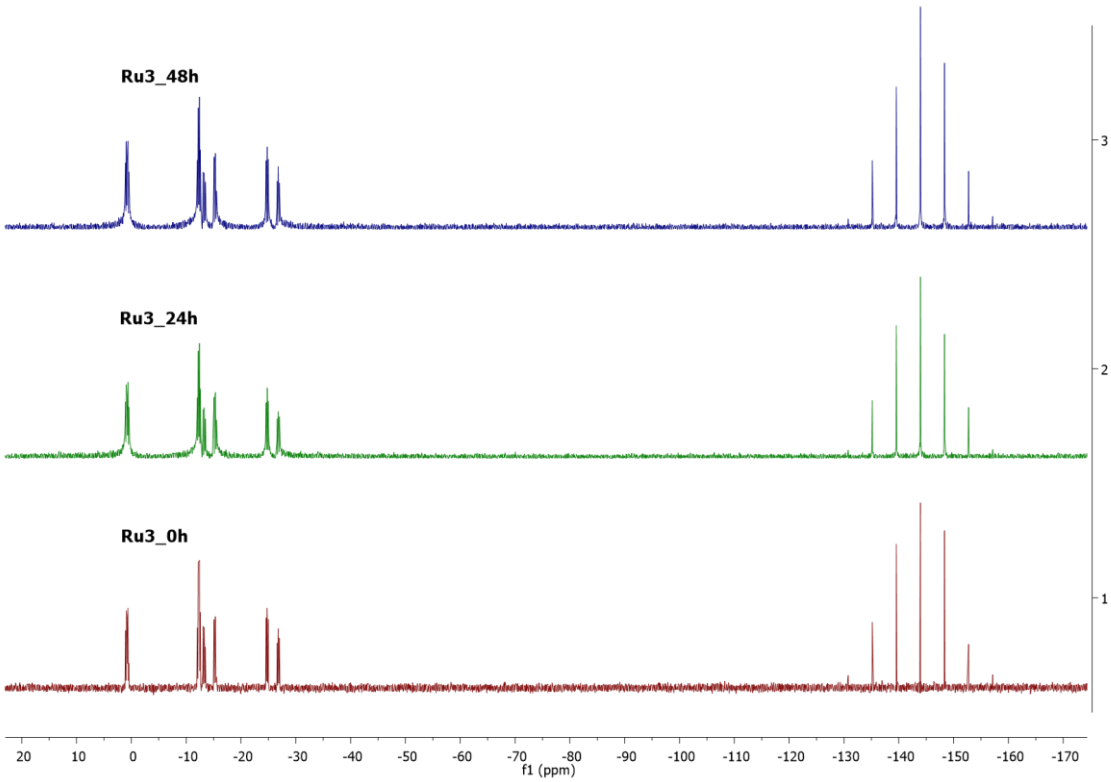


**Fig. S31** $^{31}P\ \{^{1}H\}$ NMR spectra of complex $[Ru(dmp)(dppm)_2]PF_6$ (**Ru3**) in DMSO/DMEM (90:10) at different times: 0 h, 24 h and 48 h.

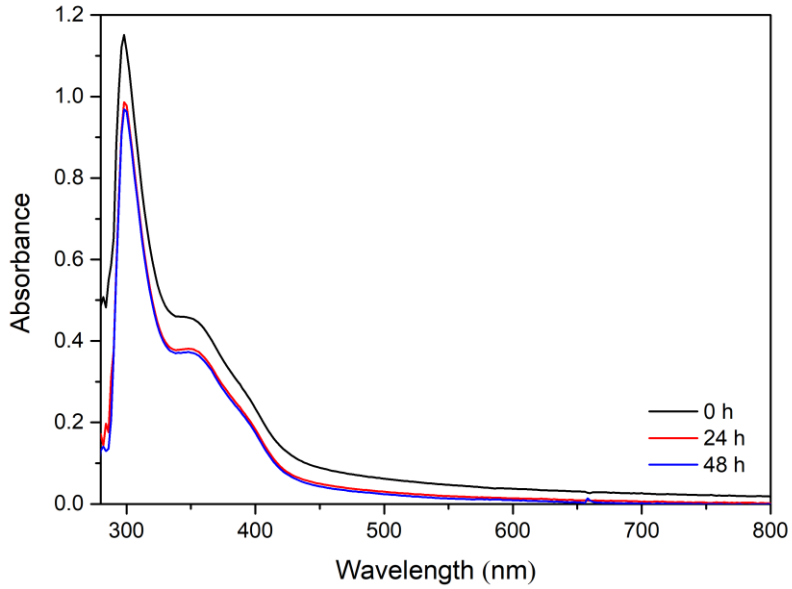


**Fig. S32** UV-Vis spectra of $[Ru(mtz)(dppm)_2]PF_6$ (**Ru1**) in DMEM containing 5 % of DMSO at different times: 0 h, 24 h and 48 h.

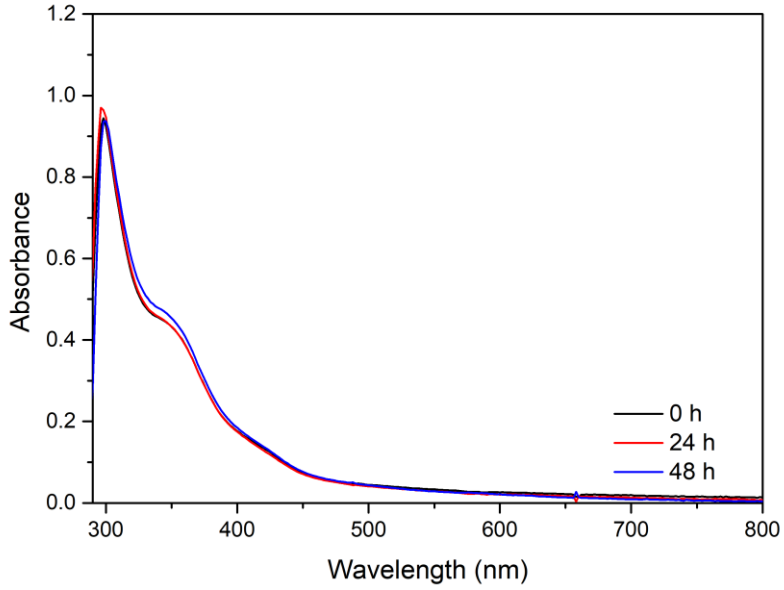


**Fig. S33** UV-Vis spectra of $[Ru(mmi)(dppm)_2]PF_6$ (**Ru2**) in DMEM containing 5 % of DMSO at different times: 0 h, 24 h and 48 h.

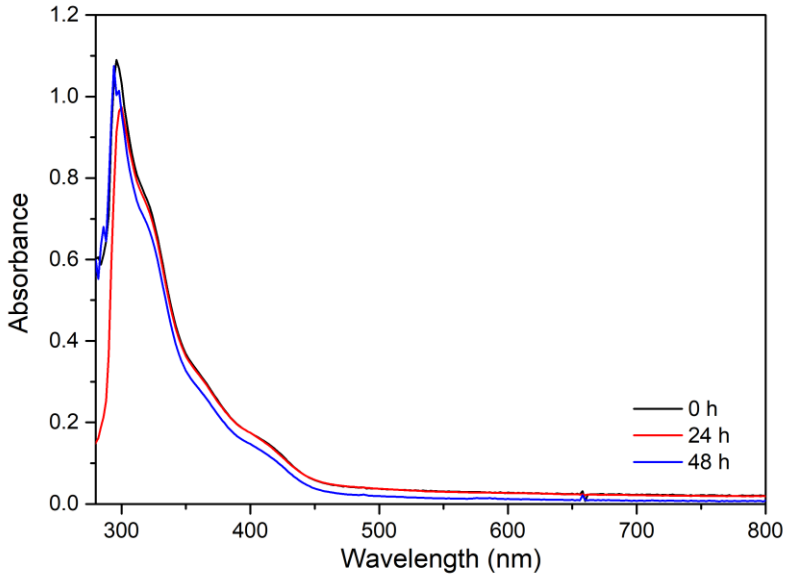


**Fig. S34** UV-Vis spectra of $[Ru(dmp)(dppm)_2]PF_6$ (**Ru3**) in DMEM containing 5 % of DMSO at different times: 0 h, 24 h and 48 h.